916 Northward Ageostrophic Winds Associated with a Tropical Cyclone

Kazuo Saito*
Meteorological Research Institute, Tsukuba, Japan

1. INTRODUCTION

It is well-know that heavy rainfalls in Japan often occur when a typhoon or tropical depression exists on the sea south of Japan. Figure 1 shows the examples, the Tokai heavy rainfall in 2000 and a heavy rainfall event in western Japan occurred in September 2013.

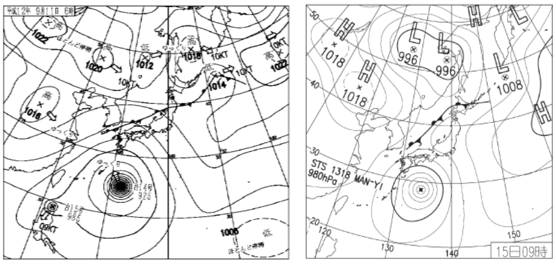

Fig. 1. Surface weather map. Left) 2100 UTC Sep 10, 2000, for the case of the Tokai Heavy rainfall. Right) 0000 UTC, Sep 15, for the case of the 2013 heavy rainfall in western Japan.

These phenomena, so-called pre-typhoon precipitation (PRE), are sometimes explained by a 'remote effect' of the typhoon, the northward moisture transport from the tropical cyclone to Japan (Fig. 2).

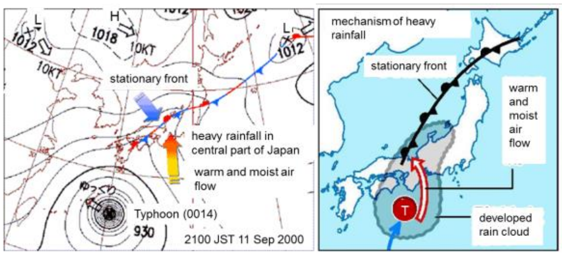

Fig. 2. Schematic explanations of the 'remote effect' of the typhoon on precipitation over Japan. Left) For the case of the Tokai Heavy rainfall. Reproduced from the homepage of the Japan Meteorological Agency (JMA, 2013). Right) For the case of the 2013 heavy rainfall in western Japan. Reproduced from the homepage of the Japan Weather Association (JWA, 2013).

However, the *northward emission* from the typhoon violates the relationship of geostrophic wind, where the direction of geostrophic wind must be parallel to the height contour, thus the outward emission from the typhoon *acrossing* the contours is impossible in geostrophic wind.

**Corresponding author address:* Kazuo Saito, Meteorological Research Institute, Forecast Research Dept., Tsukuba, Ibaraki 305-0052, Japan; e-mail: ksaito@mri-jma.go.jp

To the best of author's knowledge, the reason why the moisture is transported northward from the typhoon has not been clarified. As shown in later, distinct ageostrophic winds are sometimes observed over Japan in such the cases, but the cause are also not well-known, even by the local meteorologists.

2. Ageostrophic wind observed with typhoon Melor (0918)

Typhoon Melor (0918) made landfall in central Japan on 8 Sep 2009. The typhoon caused 6 death and 135 injured, flood above floor level 538 and below flow level 2,865. Storm surge exceeding the 4 m seawall occurred in Toyohashi, and several tornados occurred in Ibaraki and Chiba prefectures. The track of the typhoon and the surface weather map at 1200 UTC 6 October 2009 are shown in Fig. 3.

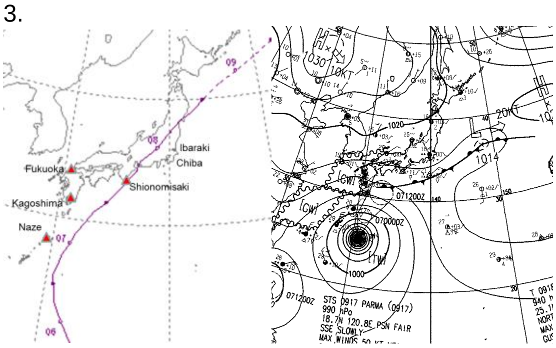

Fig. 3. Left) Track of Typhoon Melor (0918). Numerals show the date and the positions at 0000 UTC. Right) Surface weather map at 1200 UTC 6 October 2009.

When the typhoon approached Japan, distinct ageostrophic southerly winds were observed over western part of Japan. Figures 4a-c show 300 hPa height field by the JMA operational global analysis and observed winds at the aerological observatories of JMA from 0000 UTC 6th to 0000 UTC 7th October 2009. At 0000 UTC 6th (Fig. 4a) the typhoon was located far south of Kyushu, and the upper winds over Japan were west-southwesterly. While the typhoon moved northward, the upper winds over Japan changed their directions gradually from west-southwesterly to southwesterly (Fig. 4b).

At 0000 UTC 7th the typhoon approached about 300 km south of Kyushu. Aerological observations at western part of Japan (e.g., Kagoshima, Fukuoka and Shionomisaki) showed southerly or south-southwesterly winds which across the height contours. Note that a westerly wind toward the typhoon center was observed at Naze, just west of the typhoon (Fig. 4c). At 500 hPa level (Fig. 4d), winds over southern coastal area are more southerly.

Considerable rainfall was observed over southern part of Japan along a stationary front at that period (Fig. 5).

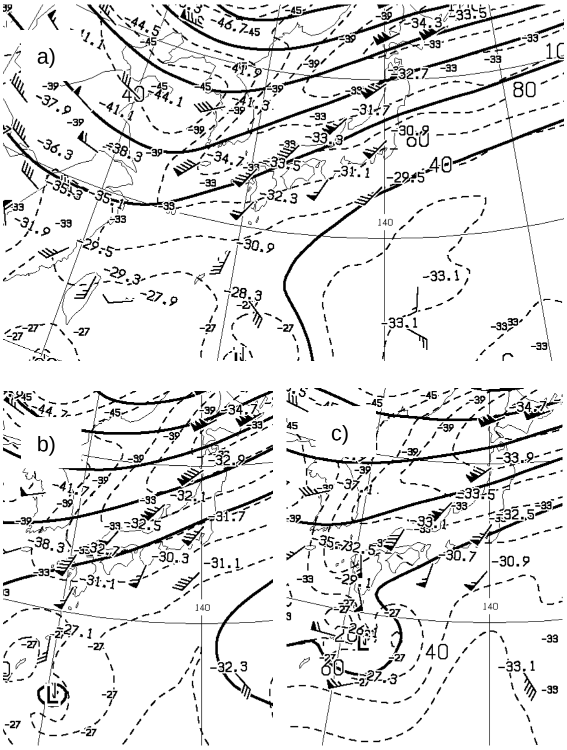

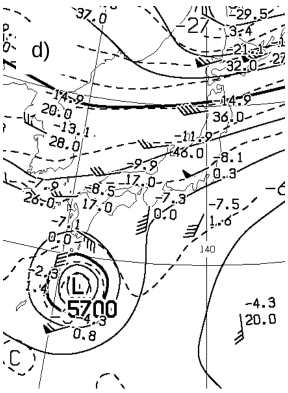

Fig. 4. a) 300 hPa height and observed winds at 0000 UTC 6 October 2009. b) Same as in a) but at 1200 UTC 6 October. c) Same as in a) but at 0000 UTC 7 October. d) Same as in c) but for 500 hPa.

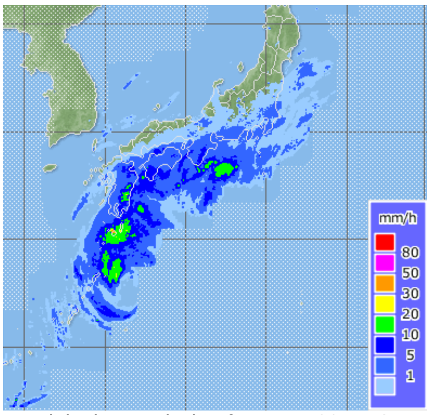

Fig. 5. Precipitation analysis of JMA at 00 UTC 7th October 2009.

As for the cause of the ageostrophic winds, Saito and Ohkado (2011) pointed out the following four possibilities:

1) Effect of low level jet caused by pressure gradient force associated with precipitation
2) Vertical momentum transport due to convective/large scale updraft
3) Orographic effects of Kyushu, Shikoku and Kii-Peninsula
4) Ageostrophic wind relating to the acceleration vector.

Here, we will consider the fourth explanation below:

Ageostrophic wind relating to the acceleration vector can be explained by the equations between the geostrophic wind components and acceleration:

$$\frac{d_g u_g}{dt} = f v_a, \quad \frac{d_g v_g}{dt} = -f u_a$$

In northern hemisphere, the direction of the ageostrophic wind is leftward of the acceleration vector (Ogura, 1978). In a usual case, when the contours around the typhoon are along concentric circles (Fig. 6), the pressure gradient force changes the direction of the wind toward the typhoon center (red arrow) and deceleration of the wind speed in the northeast quadrant directs southeastward. This deceleration makes the ageostrophic wind components u_a, negative and v_a positive (southeastward as indicated by a double arrow). Resultant wind speed becomes smaller than that of the geostrophic wind (cyclostrophic balanced wind).

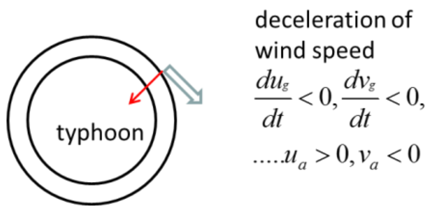

Fig. 6. Relationship between height field (solid lines), acceleration vector (red arrow) and the ageostrophic wind component (⇒).

Near the baroclinic zone, the relationship by the Sawyer (1952) and Eliassen's (1962) secondary circulation in the jet-streak four quadrant model is well known. There are some previous studies for mid-latitude troposphere jet (e.g., Shapiro and Keyser, 1990), and extratropical cyclogeneis of typhoon (Kitabatake, 2002), but this mechanism has not been used to explain the northward moisture transport relating to PRE.

When a typhoon approaches a baroclinic zone, pressure gradient force toward the typhoon center decreases between the typhoon and the baroclinic zone, and deceleration of wind speed makes the ageostrophic wind components u_a and v_a both positive in the northeast quadrant. The resultant wind becomes southerly. Near the baroclinic zone, air mass is accelerated by the jet stream eastward, and the northward ageostrophic wind v_a becomes positive. Consequently, when a typhoon approach a baroclinic zone, southerly or southwesterly winds which across the height contour is likely to prevail at both northeastern quadrant of the typhoon and its north side (Fig. 7).

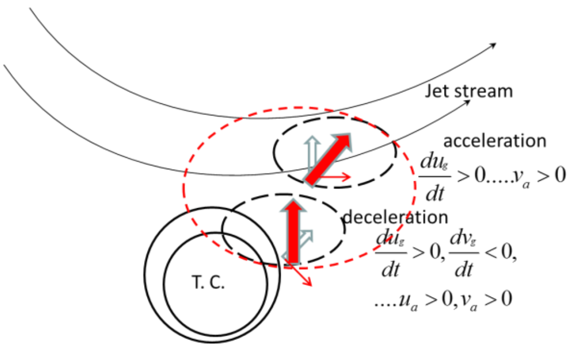

Fig. 7. Relationship between height field (solid lines), acceleration vector (red arrow), ageostrophic wind components (⇒) and resultant horizontal wind (➡).

3. Numerical experiment

3.1 Experimental design and result

We conducted a numerical experiment of this event to elucidate the cause of the ageostrophic wind. The JMA nonhydrostatic model (JMA-NHM; Saito et a; 2006; 2007) was employed as the regional NWP model with a horizontal resolution of 10 km. Initial condition is given by the JMA operational mesoscale analysis at 1800 UTC, 6 October 2009, and boundary conditions are given by the 6 hourly JMA's operational global model forecasts from 1800 UTC, 6 October (Fig. 8).

The horizontal domain size is 3,600 km x 2,880 km and the number of vertical levels is 50. Physical processes are the 3-ice bulk cloud microphysics, modified KF scheme, and MYNN level 3 closure model. These specifications are almost the same as in the JMA's operational mesoscale model (MSM) up to 2013 except the time interval of the lateral boundary condition update (in operational setting, the lateral boundary condition is updated one hourly).

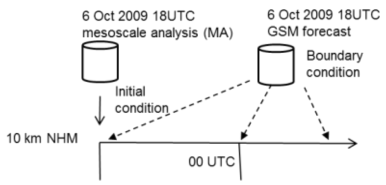

Fig. 8. Schematic chart of the numerical experiment.

Figure 9 shows surface winds and MSLP with color shade of 3-hour accumulated precipitation and the height field and horizontal winds at 500 hPa and 300 hPa predicted by JMA-NHM for 0000 UTC 7 October 2009. The observed southerly ageostrophic winds over western part of Japan are well reproduced.

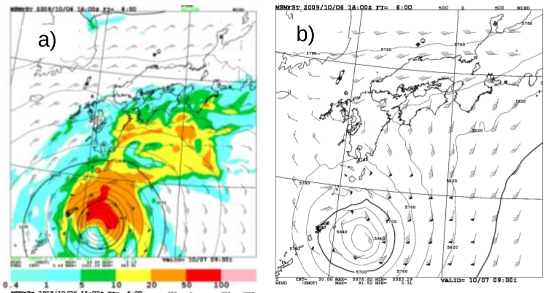

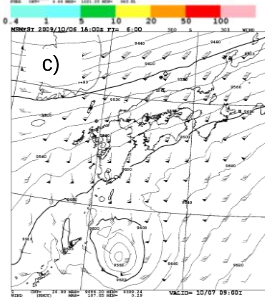

Fig. 9. a) Surface winds and MSLP with color shade of 3-hour accumulated precipitation predicted by NHM for 00 UTC 7 October 2009 (FT=6). b) Height field and horizontal winds at 500 hPa. c) Height field and horizontal winds at 300 hPa.

3.2 Analysis of ageostrophic wind component

Figure 10a and 10 b show geostrophic and ageostrophic winds at 300 hPa for 0000 UTC 7 October 2009 by JMA-NHM (FT=6). As seen in these figures, acceleration of u_g becomes negative in the northeastern quadratic of the typhoon and over Japan, and ageostrophic wind and resultant horizontal wind (Fig. 10c) in this region becomes southerly. The relationship between geostrophic and ageostrophic wind components supports the mechanism (4) that we discussed in the previous section.

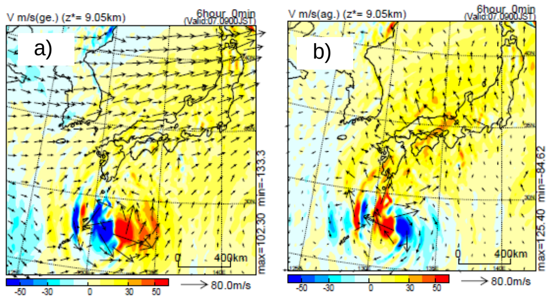

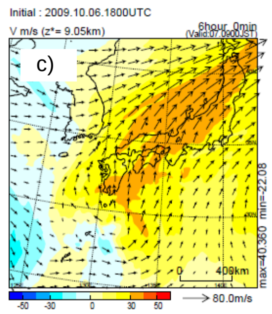

Fig. 10. a) Geostrophic wind (vectors) and its v-component (color shade) at 300 hPa for 0000 UTC 7 October 2009 by NHM (FT=6). b) Same as in a) but for ageostrophic wind and its v-component. c) Same as in a) but for horizontal wind and its v-component.

3.3 Sensitivity experiments to check other possibilities

We also conducted sensitivity tests to the precipitation process and orography in the model to check the possibility of (1)-(3). Figure 11 shows the results by a dry model, where the effect of heat release by water vapor condensation is removed. Although the northward ageostrophic winds become slightly weaker, the basic characteristic features are not different. This means that the adiabatic effect due to the precipitation may act to enhance the southerly winds over Japan but is not primary.

Figure 12 shows the geostrophic and ageostrophic winds by the experiment without orography. These patterns are very similar to Figs. 10a and 10b, and virtually no difference is seen in the horizontal wind field with and without orography (figure not shown).

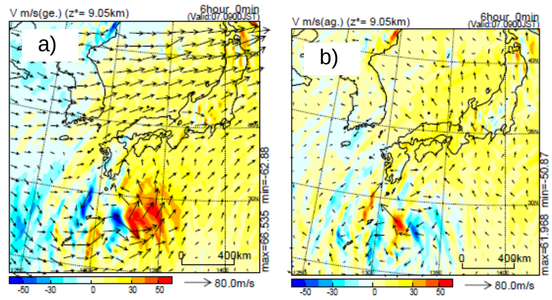

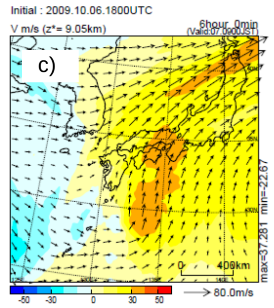

Fig. 11. Same as in Fig. 10 but results by the dry model experiment.

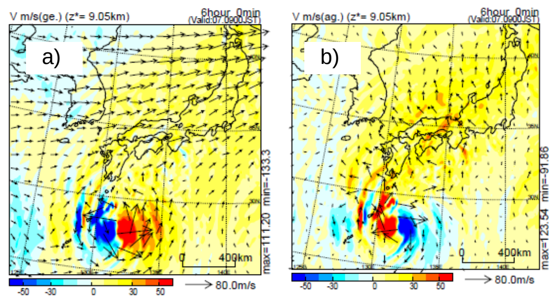

Fig. 12. Same as in Figs. 10a and b, except for the experiment without orography.

3.3. Non ax-symmetry of winds around typhoon

A similar mechanism is established in the northwestern quadrant of the typhoon, where the wind is accelerated southewestward. In this domain, ageostrophic wind directs southeastward. This explains the westerly wind just west of the typhoon center observed at Naze shown in Fig. 4c and simulated westerly wind shown in Fig. 9c.

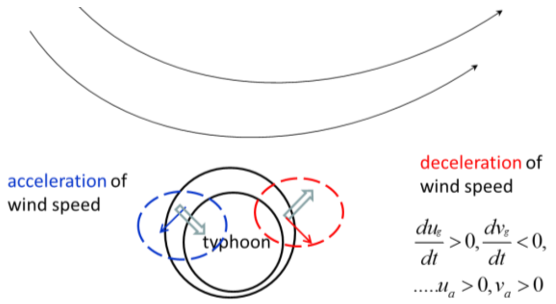

Fig. 13. Same as in Fig. 7 but relationship between the acceleration vector and ageostrophic wind in the north-western quadrant.

4. Summary

Distinct southerly ageostrophic winds were observed when typhoon Melor (0918) was located of the south coast of Japan. Numerical experiment using JMA-NHM well reproduced the northward ageostrophic wind, across the contours. This northward ageostrophic wind can be explained by dynamically induced one which directs to the leftward of the wind acceleration vector.

Effect of adiabatic process by precipitation is not negligible but small. Orography has little effect on the observed ageostrophic wind in this case.

Acknowledgments

A part of this research has been funded by MEXT Strategic Programs for Innovative Research (SPIRE). The author thanks to Yoshi Ogura for his valuable comments and encouragement. This works was inspired by Q&A in the Bulletin of Japan Meteorologists Association (Tenkist) edited by Yoshitsugu Nagasawa. Thanks are extended to Masaru Kunii and Teruyuki Kato of the Meteorological Research Institute for their helps to conduct and analyze the numerical experiment.

References

Eliassen, A., 1962: On the vertical circulation in frontal zones. *Geopfys. Publik.*, **24**, 147-160.

Ogura, Y., 1978: Dynamics of meteorology. *University of Tokyo Press*, 249pp. (in Japanese)

Kitabatake, N., 2002: Extratropical Transformation of Typhoon Vicki (9807): Structural Change and the Role of Upper-tropospheric Disturbances. *J. Meteor. Soc. Japan*, **80**, 229-247.

Saito, K., T. Fujita, Y. Yamada, J. Ishida, Y. Kumagai, K. Aranami, S. Ohmori, R. Nagasawa, S. Kumagai, C. Muroi, T. Kato, H. Eito and Y. Yamazaki, 2006: The operational JMA Nonhydrostatic Mesoscale Model. *Mon. Wea. Rev.*, **134**, 1266-1298.

Saito, K., J. Ishida, K. Aranami, T. Hara, T. Segawa, M. Narita and Y. Honda, 2007: Nonhydrostatic atmospheric models and operational development at JMA. *J. Meteor. Soc. Japan*., **85B**, 271-304.

Saito, K. and Y. Ohkado, 2011: Q&A on the inconsistency between the height contour and wind direction when a typhoon exists off the south coast of Japan. Tenkist, **71**, 10-11. (in Japanese)

Sawyer, J. S., 1952: Dynamical aspects of some simple frontal models. *Q. J. Roy. Met. Soc.*, **78**, 170-178.